

Indolo[3,2-*b*]carbazole-Based Thin-Film Transistors with High Mobility and Stability

Yiliang Wu, Yuning Li, Sandra Gardner, and Beng S. Ong*

Contribution from the Materials Design and Integration Laboratory,
Xerox Research Centre of Canada, Mississauga, Ontario, Canada L5K 2L1

Received July 21, 2004; Revised Manuscript Received October 7, 2004; E-mail: Beng.Ong@xrcc.xerox.com

Abstract: Proper functionalization of indolo[3,2-*b*]carbazole led to a new class of high-performance organic semiconductors suitable for organic thin-film transistor (OTFT) applications. While 5,11-diaryl-substituted indolo[3,2-*b*]carbazoles without long alkyl side chains provided amorphous thin films upon vacuum deposition, those with sufficiently long alkyl side chains such as 5,11-bis(4-octylphenyl)indolo[3,2-*b*]carbazole self-organized readily into highly crystalline layered structures under similar conditions. OTFTs using channel semiconductors of this nature exhibited excellent field-effect properties, with mobility up to $0.12 \text{ cm}^2 \text{ V}^{-1} \text{ s}^{-1}$ and current on/off ratio to 10^7 . As this class of organic semiconductors has relatively low HOMO levels and large band gaps, they also displayed good environmental stability even with prolonged exposure to amber light, an appealing characteristic for OTFT applications.

Introduction

Organic thin-film transistors (OTFTs) have received enormous interest in recent years as a low-cost alternative to amorphous hydrogenated silicon transistors for electronic applications.^{1–6} OTFTs are particularly suited for applications where large-area circuits (e.g., backplane electronics for large

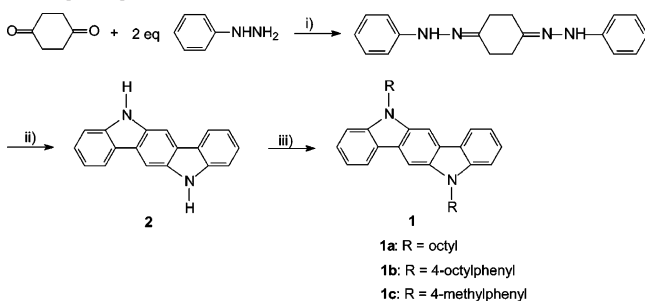
displays), desirable form factors and structural features (e.g., flexibility for e-paper), and affordability (e.g., ultralow cost for ubiquitous RFID tags) are essential. For these applications, field effect transistor (FET) mobility similar or close to that of amorphous silicon may be sufficient. To enable low-cost OTFT circuits, it is critical that useful transistor functionality be achieved under ambient fabrication conditions and that the OTFTs possess the required stability for long-term operation. However, not many organic semiconductors have both the mobility and stability to enable these practical applications. Three primary classes of p-channel organic semiconductors are noteworthy: (1) acenes such as tetracene, pentacene, and their derivatives,² (2) oligothiophenes and polythiophenes,³ and (3) fused-ring thiophene–aromatics⁴ and thiophene–vinylene/arylene derivatives.⁵ Most of these semiconductors have relatively high-lying HOMOs and narrow band gaps; they are therefore easily photooxidized, resulting in degraded semiconductor characteristics when processed in air or operated in ambient conditions. This drawback is particularly challenging for those display applications where light emission or backlight is involved. Very recently, certain oligofluorene derivatives have been reported to have high FET mobility and good stability.^{5b} We have also demonstrated that regioregular poly(3,3''-dialkylquaterthiophene)s (PQTs), solution processed under ambient conditions, afford excellent FET properties.^{3e}

Organic semiconductors based on triarylamine and carbazole structures (polymers or small molecules) have been extensively studied as hole-transport materials for optoelectronic applications (e.g., photoreceptors,⁷ organic light-emitting diodes (OLEDs),⁸ etc.) These amine-based semiconductors have the general attributes of not absorbing in the visible region of the spectrum

- (1) (a) Katz, H. E.; Bao, Z.; Gilat, S. L. *Acc. Chem. Res.* **2001**, *34*, 359–369. (b) Dimitrakopoulos, C. D.; Mascaro, D. J. *Adv. Mater.* **2002**, *14*, 99–117.
- (2) (a) Gundlach, D. J.; Lin, Y. Y.; Jackson, T. N.; Nelson, S. F.; Schlom, D. G. *IEEE Electron Device Lett.* **1997**, *18*, 87–89. (b) Kelly, T. W.; Boardman, L. D.; Dunbar, T. D.; Muryes, D. V.; Pellerite, M. J.; Smith, T. P. *J. Phys. Chem. B* **2003**, *107*, 5877–5881. (c) Sundar, V. C.; Zaumseil, J.; Podzorov, V.; Menard, E.; Willett, R. L.; Someya, T.; Gershenson, M. E.; Rogers, J. A. *Science* **2004**, *303*, 1644–1646. (d) Afzali, A.; Dimitrakopoulos, C. D.; Breen, T. L. *J. Am. Chem. Soc.* **2002**, *124*, 8812–8813.
- (3) (a) Garnier, F.; Yassar, A.; Hajlaoui, R.; Horowitz, G.; Deloffre, F.; Servet, B.; Ries, S.; Alnot, P. *J. Am. Chem. Soc.* **1993**, *115*, 8716–8721. (b) Katz, H. E.; Torsi, L.; Dodabalapur, A. *Chem. Mater.* **1995**, *7*, 2235–2237. (c) Bao, Z.; Dodabalapur, A.; Lovinger, A. J. *Appl. Phys. Lett.* **1996**, *69*, 4108–4110. (d) Sirringhaus, H.; Brown, P. J.; Friend, R. H.; Nielsen, M. M.; Bechgaard, K.; Langeveld-Voss, B. M. W.; Spiering, A. J. H.; Janssen, R. A. J.; Meijer, E. W.; Herwig, P.; de Leeuw, D. M. *Nature* **1999**, *401*, 685–688. (e) Ong, B. S.; Wu, Y.; Liu, P.; Gardner, S. J. *J. Am. Chem. Soc.* **2004**, *126*, 3378–3379. (f) Ong, B. S.; Wu, Y.; Jiang, L.; Liu, P.; Murti, K. *Synth. Met.* **2004**, *142*, 49–52.
- (4) (a) Laquindanum, J. G.; Katz, H. E.; Lovinger, A. J. *J. Am. Chem. Soc.* **1998**, *120*, 664–672. (b) Li, X.; Sirringhaus, H.; Garnier, F.; Holmes, A. B.; Moratti, S. C.; Feeder, N.; Clegg, W.; Teat, S. J.; Friend, R. H. *J. Am. Chem. Soc.* **1998**, *120*, 2206–2207.
- (5) (a) Hong, X. M.; Katz, H. E.; Lovinger, A. J.; Wang, B.; Raghavachari, K. *Chem. Mater.* **2001**, *13*, 4686–4691. (b) Meng, H.; Bao, Z.; Lovinger, A. J.; Wang, B.; Mujisce, A. M. *J. Am. Chem. Soc.* **2001**, *123*, 9214–9215. (c) Videlot, C.; Ackermann, J.; Blanchard, P.; Raimundo, J.; Frère, P.; Allain, M.; Bettignies, R.; Levillain, E.; Roncali, J. *Adv. Mater.* **2003**, *15*, 306–310.
- (6) (a) Katz, H. E.; Lovinger, A. J.; Johnson, J.; Kloc, C.; Siegrist, T.; Li, W.; Lin, Y. Y.; Dodabalapur, A. *Nature* **2000**, *404*, 478–480. (b) Facchetti, A.; Deng, Y.; Wang, A.; Koide, Y.; Sirringhaus, H.; Marks, T. J.; Friend, R. H. *Angew. Chem., Int. Ed.* **2000**, *39*, 4547–4551. (c) Babel, A.; Jenekhe, S. A. *J. Am. Chem. Soc.* **2003**, *125*, 13656–13657. (d) Bao, Z.; Lovinger, A. J.; Brown, J. J. *J. Am. Chem. Soc.* **1998**, *120*, 207–208. (e) Pappenfuss, T. M.; Chesterfield, R. J.; Frisbie, C. D.; Mann, K. R.; Casado, J.; Raff, J. D.; Miller, L. L. *J. Am. Chem. Soc.* **2002**, *124*, 4184–4185. (f) Malenfant, P. R. L.; Dimitrakopoulos, C. D.; Gelorme, J. D.; Kosbar, L. L.; Graham, T. O.; Curioni, A.; Andreoni, W. *Appl. Phys. Lett.* **2002**, *80*, 2517–2519.

(7) Law, K. Y. *Chem. Rev.* **1993**, *93*, 449–486.

(8) Casalbore-Miceli, G.; Degli Esposti, A.; Fattori, V.; Marconi, G.; Sabatini, C. *Phys. Chem. Chem. Phys.* **2004**, *6*, 3092–3096.

Scheme 1. Synthesis of 5,11-Disubstituted Indolo[3,2-*b*]carbazoles

^a Reagents and conditions: (i) AcOH/EtOH, 50 °C/1 h; (ii) concentrated H₂SO₄, 65 °C/15 min; (iii) **1a**, 1-bromooctane, aqueous 50% NaOH, benzyltriethylammonium chloride, DMSO, 50 °C/2 h; **1b**, 1-iodo-4-octylbenzene, 12-crown-6, Cu, 1,2-dichlorobenzene, reflux/24 h; **1c**, 4-iodotoluene, 12-crown-6, Cu, 1,2-dichlorobenzene, reflux/24 h.

(larger band gaps) and possessing reasonable stability against oxidative doping by atmospheric oxygen (lower lying HOMOs). However, while these materials may be satisfactory for their intended applications, most provide low FET mobility in OTFTs due to their inability to form structurally ordered semiconductor layers.

We report here our studies of a new class of OTFT semiconductors based on a tertiary diamine structure, 5,11-disubstituted indolo[3,2-*b*]carbazole **1**. Similar to triarylamine and carbazole compounds, **1** has a large band gap and lower lying HOMO than most semiconductors used in OTFTs, and is therefore expected to be environmentally far more stable. The relatively large and planar molecular structure of **1** would also permit facile establishment of higher molecular orders that are conducive to charge carrier transport. Accordingly, through strategic substitution, **1** can be transformed into an efficient charge transport system that may serve as an excellent, environmentally stable channel semiconductor for OTFTs.

Results and Discussion

Previously, we reported the use of 5,11-bis(1-naphthyl)indolo[3,2-*b*]carbazole as a hole-transporting/electron-blocking material for OLEDs.⁹ However, due to the presence of sterically encumbered naphthyl substituents, this compound lacked the ability to order and formed amorphous films upon vacuum deposition. It provided very low FET mobility when used as a channel semiconductor in OTFTs. This is not surprising since charge transport in organic semiconductors is dominated by hopping,¹⁰ and amorphous materials are not expected to give high mobility. To be an efficient semiconductor for OTFTs, the indolo[3,2-*b*]carbazole system needs to provide (i) proper molecular ordering for efficient charge carrier transport and (ii) sufficient stabilization to radical cations (i.e., hole carriers) to enable efficient hole injection. Accordingly, an indolo[3,2-*b*]carbazole system such as **1b** (Scheme 1), which has two strategically placed long alkyl chains to induce molecular self-assembly^{3a,e} and two conjugated triarylmino hole-receptor sites capable of providing resonance stabilization to injected holes, would be an ideal semiconductor system for OTFTs. Indolo[3,2-*b*]carbazoles **1a** and **1c** were also synthesized for studies to validate our hypothesis on the structure–property correlation

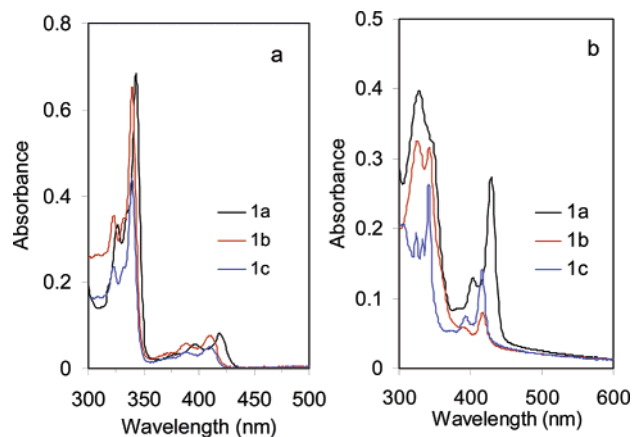


Figure 1. UV–vis absorption spectra of indolo[3,2-*b*]carbazoles **1**: (a) dilute solutions in chloroform and (b) thin films.

for this structural series. **1a** has two octyl chains but without the intervening phenylene moieties to provide added resonance stabilization to radical cations, while indolo[3,2-*b*]carbazole **1c** has the “radical cation-stabilizing” phenylene moieties but without the octyl side chains to promote molecular ordering.

A general synthesis of indolo[3,2-*b*]carbazole **1** is illustrated in Scheme 1. The parent indolo[3,2-*b*]carbazole, **2**, was prepared via condensation of 1,4-cyclohexanedione with 2 molar equivalents of phenylhydrazine to form cyclohexane-1,4-dione bis(phenylhydrazine), followed by double Fischer indolization.¹¹ 5,11-Dialkylindolo[3,2-*b*]carbazole, such as **1a**, was readily prepared by phase-transfer condensation of **2** with alkyl bromide and aqueous NaOH in DMSO in the presence of a phase-transfer catalyst, benzyltriethylammonium chloride. 5,11-Diarylindolo[3,2-*b*]carbazoles such as **1b** and **1c**, on the other hand, were obtained by Ullmann condensation of **2** with the corresponding aryl iodides using excess copper and a catalytic amount of 18-crown-6 in refluxing 1,2-dichlorobenzene. The 5,11-disubstituted indolo[3,2-*b*]carbazoles **1a**, **1b**, and **1c** are soluble in organic solvents such as toluene, chloroform, and chlorobenzene.

The UV–vis spectrum of a dilute solution of **1a** in chloroform showed absorption peaks at 419, 396, and 343 nm, while those of **1b** and **1c** showed absorption peaks at 410, 388, and 340 nm (Figure 1a). The spectral absorptions of vacuum-deposited thin films of **1** were slightly red shifted, with absorption maxima at 428, 400, and 327 nm for **1a**, 415, 341, and 323 nm for **1b**, and 415 and 341 nm for **1c** (Figure 1b). The optical band gaps estimated from the absorption edges of the thin-film spectra are, respectively, 2.65, 2.8, and 2.8 eV for **1a**, **1b**, and **1c**. These are larger than those of most organic semiconductors used in OTFTs.^{2–5} Semiconductors of this nature with large band gaps, which absorb in the UV or near-UV regions are suitable for fabricating transparent OTFT circuits which would be useful for optoelectronic devices requiring circuit transparency.¹² Cyclic voltammetric measurements of **1b** in 0.1 M Bu₄ClO₄/CH₂Cl₂ solution showed a reversible oxidation process with an onset oxidation potential at 0.74 eV against a Ag/AgCl electrode, corresponding to an estimated HOMO level of 5.12 eV from vacuum. This is lower than those of most regioregular polythiophenes (4.9–5.0 eV),^{3e,f} thus indicating higher oxidative stability.

(9) Hu, N.; Xie, S.; Popovic, Z.; Ong, B.; Hor, A. *J. Am. Chem. Soc.* **1999**, *121*, 5097–5098.
(10) Horowitz, G.; Delannoy, P. In *Handbook of Oligo- and Polythiophenes*; Fichou, D., Ed.; Wiley-VCH: Weinheim, Germany, 1999; pp 283–316.

(11) Robinson, B. *J. Chem. Soc.* **1963**, 3097–3099.
(12) Nomura, K.; Ohta, H.; Ueda, K.; Kamiya, T.; Hirano, M.; Hosono, H. *Science* **2003**, *300*, 1269–1272.

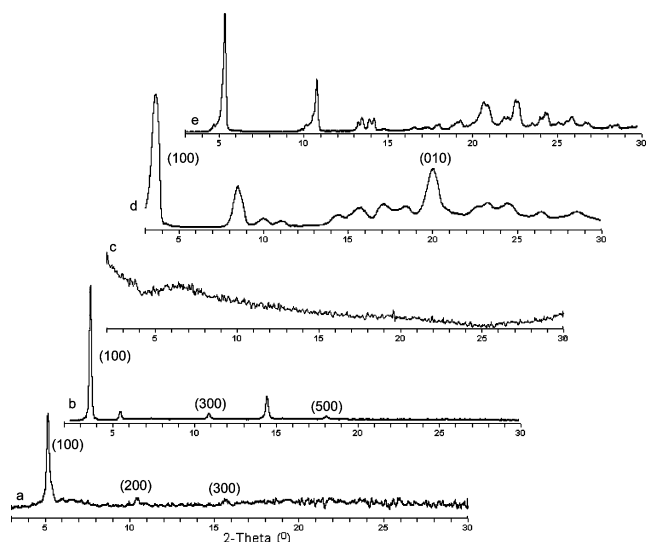


Figure 2. X-ray diffraction patterns of (a) a vacuum-deposited thin film of **1a**, (b) a vacuum-deposited thin film of **1b**, (c) a vacuum-deposited thin film of **1c**, (d) a powder of sublimed **1b**, and (e) a powder of **1b** recrystallized from toluene.

As expected, both **1a** and **1b** formed highly crystalline thin films upon vacuum deposition on a glass substrate with sharp diffraction peaks in their X-ray diffraction (XRD) patterns. On the other hand, only featureless broad diffraction peaks were present in the thin-film XRD pattern of **1c**, indicating its amorphous nature as a result of its inability to undergo proper molecular organization in the thin film. These results unequivocally affirmed the critical role of long alkyl side chains (e.g., octyl chains) in the molecular self-assembly of indolo[3,2-*b*]-carbazole compounds during vacuum deposition. The thin-film XRD pattern of **1a** (Figure 2a) displayed a primary diffraction peak at $2\theta = 5.24^\circ$ (d -spacing 16.85 Å), with the second- and third-order diffraction peaks at $2\theta = 10.48^\circ$ and 15.80° . On the other hand, the thin-film XRD pattern of **1b** (Figure 2b) showed stronger diffraction intensities, with the primary diffraction peak appearing at $2\theta = 3.62^\circ$ (d -spacing of 24.41 Å). Sharp diffraction peaks up to the fifth order were observed (third- and fifth-order diffraction peaks at $2\theta = 10.91^\circ$ and 18.09° , respectively), indicating a high degree of ordering and crystallinity. The intense diffraction peak at $2\theta = 20.02^\circ$ (d -spacing 4.4 Å) in powder XRD of **1b** (Figure 2d) is likely due to the π - π stacking order. Compared to this powder XRD pattern, the absence of many reflections, particularly π - π stacking reflections, in thin-film XRD patterns of **1a** and **1b** indicates that the molecules preferentially adopted an “edge-on” orientation relative to the substrate. This led to the formation of layered structures with interlayer distances of 16.85 and 24.41 Å for **1a** and **1b**, respectively. This type of edge-on orientation with the π - π stacking direction parallel to the substrate is known to be favorable for in-plane charge transport.^{3d} On the basis of two fully extended peripheral side chains tilted at an angle of approximately 25° against the indolocarbazole molecular plane,⁹ the molecular heights of **1a** and **1b** were estimated to be, respectively, about 24 and 30 Å. Thus, the observed shorter interlayer distances would suggest that either the molecules had an inclining orientation with respect to the substrate or the interlayer involves some interdigitation of side chains of the molecules in the adjacent layers. The diffraction peak of **1b** at $2\theta = 5.48^\circ$ in the thin-film XRD pattern may be due to a

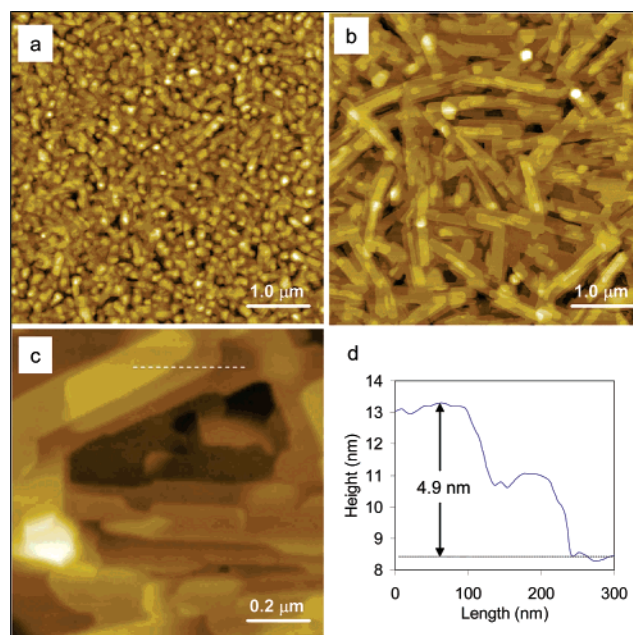


Figure 3. AFM topographic images of **1b**: (a) vacuum-deposited film on a substrate at 25°C , (b) vacuum-deposited film on a substrate at 50°C , (c) blown-up image from (b) showing terrace-like layered structures, and (d) step heights of crystalline terrace layers as measured by a profiler along the dotted line direction in (c).

different crystal structure. Through comparison of the powder XRD patterns of **1b** from a sublimed sample (Figure 2d) and a recrystallized sample (Figure 2e), it is apparent that they did not have the same crystal structures. The primary diffraction peak of the sublimed sample appeared at $2\theta = 3.62^\circ$, while that of the recrystallized sample appeared at $2\theta = 5.48^\circ$. Accordingly, compound **1b** may exist in different crystal forms depending on the crystallization and deposition conditions. Preliminary X-ray results of a single crystal of **1b** gave a very complex diffraction pattern, manifesting its polycrystalline nature. Definitive assignment of the crystal structures will require further crystallographic studies of carefully grown crystals under well-controlled crystallization and deposition conditions.

The crystalline structures in the vacuum-deposited thin films of **1b** at different substrate temperatures can be directly visualized through the AFM technique. Parts a and b of Figure 3 are the AFM topographic images of **1b** vacuum-deposited on an octyltrichlorosilane (OTS-8)-treated SiO_2 surface at two different substrate temperatures. Small crystal grains of average diameter of about 100–200 nm were observed in the thin film deposited at a substrate temperature of 25°C . The crystal grains grew in size with increasing substrate temperature, and at 50°C , they were relatively large and elongated in shape, with the average grain size being about $0.2\ \mu\text{m} \times 1\ \mu\text{m}$. These crystal grains showed terrace-like layered structures, with the layers lying parallel to the SiO_2 surface (Figure 3c). A cross-section of a terraced crystal structure gave step heights of about 2.45 nm, which are identical to the interlayer distance extracted from XRD data.

To study the FET properties of indolo[3,2-*b*]carbazole semiconductors **1**, a bottom-gate, top-contact OTFT with a 100 nm vacuum-deposited channel semiconductor was utilized as our test device structure. All three indolo[3,2-*b*]carbazole compounds displayed p-type accumulation FET behaviors when

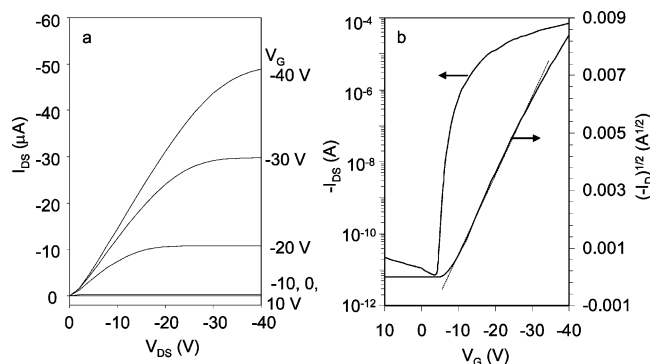


Figure 4. FET characteristics of an exemplary OTFT with vacuum-deposited **1b** (substrate at 50 °C, channel length 90 μm, channel width 5000 μm): (a) output curves at different gate voltages and (b) a transfer curve in the saturated regime at a constant source-drain voltage of −40 V and square root of the absolute value of the current as a function of the gate voltage.

Table 1. FET Mobility and Current On/Off Ratio of OTFTs with **1b** Semiconductor Layers Deposited at Various Substrate Temperatures (T_d)

T_d (°C)	mobility ($\text{cm}^2 \text{V}^{-1} \text{s}^{-1}$)	on/off ratio
25	0.01–0.02	10^5 – 10^6
50	0.07–0.12	10^6 – 10^7
70	0.007–0.01	10^5

used as channel semiconductors in OTFTs. With the semiconductors deposited at a substrate temperature of 25 °C, the observed FET mobility follows the order **1b** > **1a** \gg **1c**. As expected, **1c** provided the lowest mobility ($1.0 \times 10^{-5} \text{ cm}^2 \text{ V}^{-1} \text{ s}^{-1}$) in this series, and no improvements in FET performance even at substrate temperatures up to 70 °C. The observed low mobility of **1c** was obviously due to its lack of appropriately long alkyl side chains to induce molecular organization during vacuum deposition. On the other hand, **1a**, which has two peripheral octyl side chains, yielded higher crystallinity in thin films, and thus higher FET mobility ($(1.3\text{--}3.0) \times 10^{-3} \text{ cm}^2 \text{ V}^{-1} \text{ s}^{-1}$) in OTFTs. The mobility of **1a** was nonetheless still low as this structure is devoid of aryl substituents at the 5,11-positions to provide the needed resonance stabilization to injected hole carriers. In line with these considerations, we observed that the OTFTs with **1b** semiconductor, which has *N,N*-bis(4-octylphenyl) substitutions, exhibited the highest mobility ($0.01\text{--}0.02 \text{ cm}^2 \text{ V}^{-1} \text{ s}^{-1}$). This is the manifestation of the ability of **1b** to self-organize through the octyl side-chain interactions and to provide sufficient resonance stabilization via phenylene substituents.

As noted, the FET performance of **1b** varied with the substrate temperature, and optimum performance was achieved when **1b** was deposited at a substrate temperature of 50 °C (Table 1). The FET behaviors of such a device (Figure 4) conform well to the conventional transistor models in both the linear and saturated regimes. The output curve shows very good saturation behaviors with clear saturation currents. The device gave a mobility up to $0.12 \text{ cm}^2 \text{ V}^{-1} \text{ s}^{-1}$ and a current on/off ratio up to 10^7 , with a threshold voltage of −7 V and a subthreshold swing of 1 V dec^{-1} . These are among the best overall OTFT properties reported. A slight contact resistance, due to the energetic mismatch between the semiconductor and electrode materials, was however observed. The OTFTs fabricated at substrate temperatures higher than 50 °C showed decreased

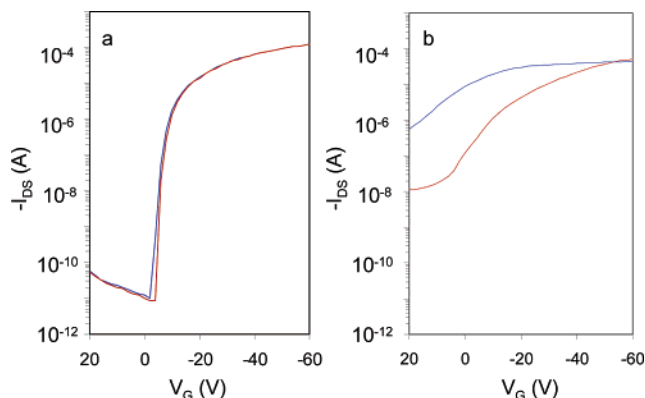


Figure 5. Transfer characteristics of OTFTs (channel length 90 μm, channel width 5000 μm, $V_{DS} = -60 \text{ V}$) in the saturated regime with (a) **1b** as the channel semiconductor deposited at a substrate temperature of 50 °C and (b) HT-P3HT as the channel semiconductor spin coated from a 0.7 wt % solution in chlorobenzene at ambient conditions. Transfer curves were obtained in the dark (red line) and then measured under white light (blue line).

mobility and current on/off ratio. Similar to what has been seen in many OTFTs (e.g., pentacene TFTs),^{2a,b} the variation in FET performance of **1b** with substrate temperature was related to the change in crystal grain size as noted by AFM analysis; i.e., larger crystal grains yielded higher mobility and current on/off ratio. As with most other solution-processable organic semiconductors (e.g., oligothiophenes),^{3a,b} the devices with the solution-deposited semiconductor of **1b** also gave reduced mobility ($\sim 7.0 \times 10^{-3} \text{ cm}^2 \text{ V}^{-1} \text{ s}^{-1}$) and on/off ratio (5×10^5).

An appealing attribute of indolo[3,2-*b*]carbazole semiconductors such as **1b** is their environmental stability. They exhibited much better air and photochemical stability than most common organic semiconductors reported to date. For example, the transfer characteristics of OTFTs with **1b** semiconductor deposited at a substrate temperature of 50 °C (Figure 5a) were found to be essentially the same in ambient conditions when the measurements were carried out in the dark and under white light. The current on/off ratio was $\sim 10^7$ in both cases, demonstrating the excellent stability of **1b** against oxidative doping or photochemical degradation. The devices were also relatively stable over an extended period of time in air under amber light exposure. Our earlier OTFTs fabricated with **1b** at a substrate temperature of 25 °C had shown only a slight decrease in mobility (from $0.01\text{--}0.02$ to $0.007\text{--}0.01 \text{ cm}^2 \text{ V}^{-1} \text{ s}^{-1}$) and current on/off ratio (from $10^5\text{--}10^6$ to $10^4\text{--}10^5$) after continuous exposure to amber light in ambient conditions for more than one year. For comparison, the FET performance of OTFTs with the well-known regioregular head-to-tail poly(3-hexylthiophene) semiconductor (HT-P3HT) was found to be very sensitive to air, particularly on exposure to light. When measured in air in the dark, the HT-P3HT devices gave an average initial current on/off ratio of about 10^3 , but the current on/off ratio dropped to less than 10^2 when the measurements were carried out under white light. On exposure to amber light in air, the HT-P3HT devices rapidly degraded in performance, with their current on/off ratio dropping from 4000 to 10 over a period of just 8 h.

Conclusion

We have demonstrated that properly functionalized indolo[3,2-*b*]carbazoles **1** represent a new class of high-performance

p-channel semiconductors with good environmental stability for organic electronic applications. To achieve high FET mobility, two critical features need to be present in the indolo[3,2-*b*]-carbazole structure: (i) a functionality, such as 5,11-diaryl substitution, that is capable of providing sufficient resonance stabilization to injected hole carriers (radical cations) and (ii) appropriately long peripheral alkyl side chains to promote molecular self-organization. Another appeal of 5,11-diarylindolo[3,2-*b*]carbazoles as channel semiconductors for OTFTs is their environmental stability owing to their relatively low-lying HOMOs and large band gaps. We anticipate further FET

performance improvements will be made through structural and device fabrication optimizations.

Acknowledgment. Partial financial support is provided by the National Institute of Standards and Technology through an Advanced Technology Program Grant (70NANB0H3033).

Supporting Information Available: Instrumentation, materials synthesis and characterization, and OTFT fabrication and evaluation (PDF). This material is available free of charge via the Internet at <http://pubs.acs.org>.

JA0456149